FOUR-OCTAVE SIX-PORT RECEIVER AND ITS CALIBRATION FOR BROADBAND COMMUNICATIONS AND SOFTWARE DEFINED RADIOS

C. de la Morena-Álvarez-Palencia and M. Burgos-García

Microwave and Radar Group
Department of Signals, Systems and Radiocommunications
Escuela Técnica Superior de Ingenieros de Telecomunicación
Technical University of Madrid, Madrid 28040, Spain

Abstract—This paper presents a software defined radio six-port receiver for a novel broadband mobile communications system. The prototype covers the frequency range from 0.3 GHz to 6 GHz, and operates with up to 100 MHz-wide channels. The multi-band and multi-mode demodulation capabilities of the six-port architecture have been experimentally demonstrated. The six-port receiver has been satisfactorily proved for high data rates (up to 93.75 Mb/s, limited by the available test instruments). An efficient six-port auto-calibration method suitable for large instantaneous bandwidth systems is presented and validated.

1. INTRODUCTION

The Software Defined Radio (SDR) is thought to play an important role in future communication systems, due to its reconfiguration and multi-mode operation capabilities. These features enable to change the system functionality without any change in the hardware. The original idea of a SDR hardware implementation consisted of placing the ADC (Analog to Digital Converter) just at the output of the antenna [1]. However, this implementation is currently impossible, due to the ADC limitations. In practice, the SDR hardware is composed of a reconfigurable baseband digital signal stage and a broadband radio frequency (RF) front-end. But the design of a general-purpose broadband RF front-end, with multi-mode and reconfiguration features, is not a simple matter.

In the search of a universal and flexible radio platform, capable of operating with multiple standards in multiple bands, several RF architectures have been studied [2–4]. Two of the best candidates to implement a SDR are the direct frequency conversion architecture, also named zero-IF, and the low-IF architecture. These structures have many advantages suitable for SDR, such as flexibility, reconfigurability, low-cost, and high level of integration, but their main problems derive from the I-Q mod/demodulator devices. The trend towards high data rates services will require larger bandwidths, which become possible at high frequencies. I-Q mod/demodulators cannot operate in very large frequency ranges, so the use of zero-IF and low-IF architectures is limited by these devices. Six-port network is an interesting direct conversion architecture that is nowadays emerging as a promising alternative [4–7], as it does not use I-Q mixers for the frequency conversion. The main characteristic of the six-port architecture is its extremely large bandwidth, which involves multi-band and multi-mode capabilities. Six-port networks can operate at very high frequencies, being a serious alternative for millimetre-wave frequencies and large relative-bandwidth applications [7–9]. But since the six-port receiver is said to be a good solution for the multi-band demodulation of high-speed signals, not many experimental demodulation results have been published up to now. This paper demonstrates empirically and quantitatively the wideband behaviour of the six-port architecture, and the capability of performing high data rates. A new real-time six-port auto-calibration method for high data rates applications is also presented and experimentally validated.

2. FUNDAMENTALS OF THE SIX-PORT RECEIVER

The origin of the six-port network dates from the seventies, when it was introduced as an alternative network analyzer [10]. The principle of operation of the six-port receiver is based on the measurement

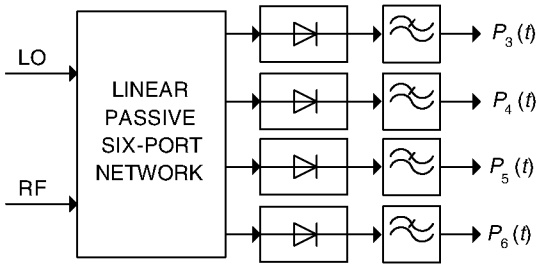

Figure 1. Block diagram of six-port receiver.

of four independent powers, when the local oscillator (LO) and RF signals are introduced into the remaining two ports [11]. A six-port receiver consists of a linear and passive six-port network and four power detectors, as it is shown in Figure 1.

Original I-Q components are regenerated from the four power observations and some constant parameters depending on system response, known as calibration constants. General demodulation equations in six-port receivers are expressed as follows:

$$I(t) = \sum_{i=3}^{6} h_i P_i(t) \tag{1}$$

$$Q(t) = \sum_{i=3}^{6} n_i P_i(t) \tag{2}$$

where h_i and n_i are the calibration constants. A calibration process is required to calculate them. Physical calibration methods use external physical standards terminals to calibrate the system. Nevertheless, this procedure is impractical for a six-port receiver. Real-time calibration methods are more suitable, as they can be performed while the system is operating. In Section 4 we present a real-time auto-calibration method, specially suited for broadband and high data rate applications.

3. DESCRIPTION OF THE SIX-PORT RECEIVER

The objective is to develop a reconfigurable radio front-end for broadband mobile applications. Nowadays, the aim of a SDR for mobile applications can be reduced to receive every standard up to 6 GHz, as all cellular and WLAN communications are located in that frequency range. Consequently, we have implemented a 698–5850 MHz (three-octave) six-port receiver prototype. The system can operate with broadband signals, up to 100 MHz-wide signals, and different modulation schemes.

The six-port network topology is represented in Figure 2. This is a typical six-port configuration, composed of three 90-degrees hybrid couplers and a Wilkinson power divider. Output six-port signals are combinations of the input RF and LO signals with different relative phase shifts of 0, $\pi/2$, $-\pi/2$, and π rad.

The design of the 90-degrees hybrid couplers is the most difficult part, as a three-octave tight coupler is required. Branch-line and rate-race couplers are suitable for obtaining tight coupling values, such as 3 dB. However, these couplers are inherently narrowband circuits ($< 20\%$ bandwidth). The use of 3 dB Lange couplers enhances the

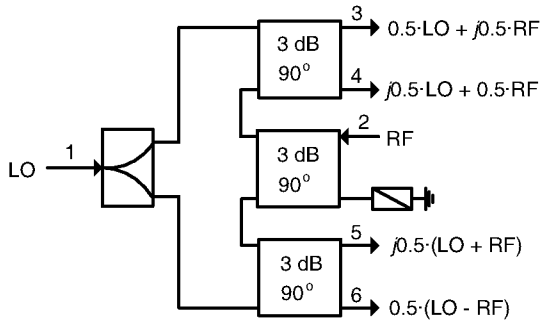

Figure 2. Six-port network topology.

bandwidth, but only up to one octave. A tight coupler can also be obtained by connecting two couplers in tandem. A three-octave 3 dB coupler can be obtained from the tandem connection of two 8.34 dB multisection couplers. However, such large bandwidth will require a high coupling level of the central section, and edge-coupled structures do not provide coupling levels higher than 8 dB. Broadside-coupled lines are more suitable, as they achieve coupling levels up to 2 or 3 dB. Consequently, we have implemented a seven section 3 dB tandem coupler with broadside-coupled striplines. Its maximum phase and amplitude imbalances are 4° and 1.2 dB over the entire frequency range. The power divider used is LYNX 111.A0214, whose characteristics are: 0.5–6 GHz frequency range, 0.8 dB insertion loss, 18 dB isolation, ± 0.2 dB amplitude imbalance and $\pm 3°$ phase imbalance. The detailed description of the six-port network design is described in [12].

The design criterion of a six-port junction consists of achieving a good distribution of the q_i-points [10]. In general, the closer the magnitudes of q_i, and the larger the differences between the arguments of q_i, the better will be the performance of the circuit. Nevertheless, the six-port network can provide good results even when the ratios of the magnitudes of q_i are greater than 4, and the phase differences between q_i are smaller than 25° [13]. When RF and LO input ports are completely isolated, the equivalent q_i-points of the six-port network can be expressed in terms of scattering parameters as:

$$q_i = -\frac{s_{i1}}{s_{i2}}; \quad i = \{3, 4, 5, 6\} \tag{3}$$

Ideally, in our six-port network topology (Figure 2) the magnitudes of q_i-points are equal to 1, and the arguments differ 90 degrees. The measured q_i-points of the developed six-port network satisfactorily fulfill these requirements, as it can be seen in Figure 3.

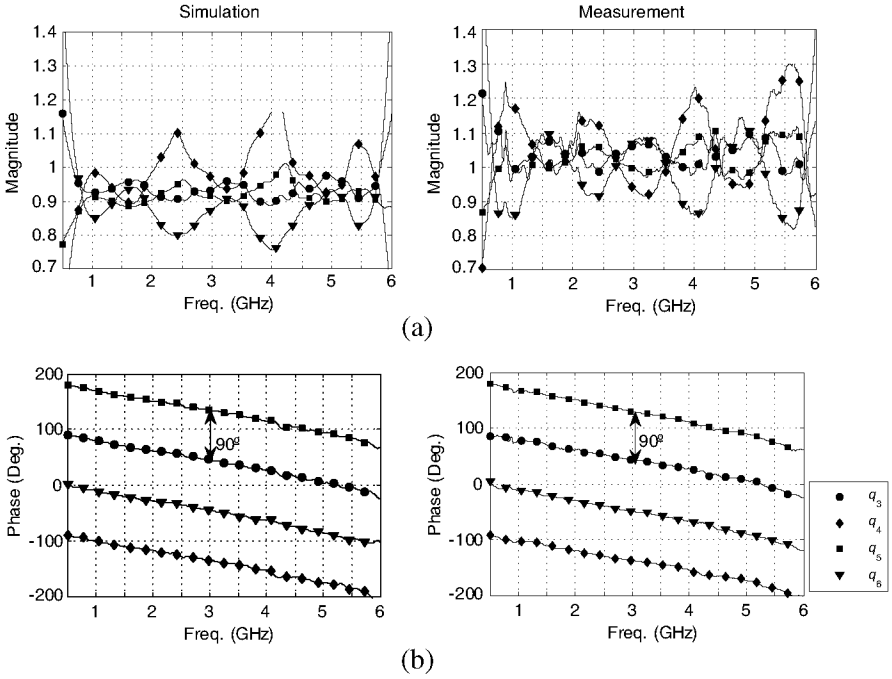

Figure 3. Simulated and measured q_i-points of the six-port network. (a) Magnitudes. (b) Phases.

The magnitudes of q_i are in the range of 0.7 to 1.5 from 500 MHz to 6 GHz, and the maximum error in the relative phase differences is 10° over the theoretical 90°. Therefore, according to [13], the operating frequency range of the six-port network could be enlarged, as it will be demonstrated in Section 5.2.

The six-port network prototype can be seen in Figure 4. The three 3 dB couplers have been assembled over a metallic structure. They are interconnected by external coaxial cables, which must have the same length in order to preserve the six-port phase behaviour. The power divider, although it does not appear in the photograph, is connected to the couplers by two coaxial cables, which must be identical in length. However, the two cables connecting the power divider to the couplers do not have to be identical in length to the cables interconnecting the couplers, since what it has to be maintained is the four relative phase shifts of 0, $\pi/2$, $-\pi/2$, and π rad.

The overall receiver includes a power detector, a low-pass filter and a video amplifier at each six-port network output, implemented

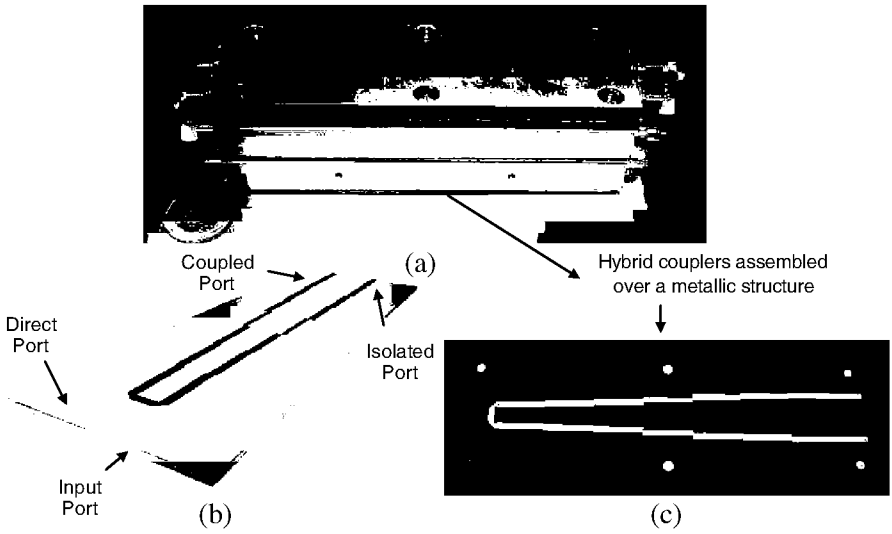

Figure 4. Six-port network prototype. (a) External appearance. (b) 3D view of the 3 dB tandem coupler. (c) Fabricated 3 dB tandem coupler.

in microstrip technology ($\varepsilon_r = 2.17$ Cu-clad substrate). The power detectors are implemented with the HP HSMS-286 Schottky diode. We use a bias current in order to extend the square law behaviour, although it involves a trade off between sensitivity and square law dynamic range. A shunt 50 Ω resistor gives broadband input match, but at the expense of detection sensitivity. MiniCircuits RLP-50+ and MAR-8A+ components are used for the low-pass filters and video amplifiers, respectively. The low noise amplifier (LNA) and the automatic gain control (AGC) stage have not been included in the prototype, although these components would be necessary in a SDR front-end. Another important issue in a SDR implementation is the RF filtering to eliminate the out-of-band interference signals. But multi-band or tuneable RF filters are difficult to design over large frequency ranges. Conventional multi-band filtering techniques have consisted of filter banks, with the disadvantage of the circuit size. More advanced techniques are based on single circuits performing the multi-band filtering. Some solutions of dual-, triple- or quad-band have been proposed [14–16], and currently the efforts are focused on the design of multi-band filters with an arbitrary number of pass-bands. Microelectromechanical systems (MEMS) devices have displayed remarkable characteristics as variable devices and have been applied as tuneable or reconfigurable multi-band RF circuits [17].

Anyway, the multi-band frequency-selective filtering is a wide research area and it would deserve a separate investigation, which is far from the objective of this work.

This well-known six-port topology also allows of analog *I-Q* regeneration, although with some limitations [11]. On one hand, a perfect cancellation of the rectified wave component is required. On the other hand, the quality of the demodulated signal strongly depends on circuit imbalances. In practice, a broadband device without impairments is not realizable. Consequently, we will sample the four baseband output signals to take advantage of the digital domain. Digital *I-Q* regeneration makes it possible to compensate circuit imbalances by means of real-time calibration algorithms. This option has certainly more sense in a SDR scenario.

Currently, a new version of the six-port network based on LTCC (Low Temperature Co-fired Ceramic) technology is under development. Higher level of integration and better results could be obtained with LTCC technology, as the components can be internally interconnected, in addition to more compact size.

4. CHANNELIZED AUTO-CALIBRATION METHOD

The proposed method is based on the use of a known training sequence at the beginning of each burst to auto-calibrate the system, as described in [18]. Considering a training sequence of M symbols at the RF input port, Equations (1) and (2) can be written as:

$$\begin{bmatrix} I(1) \\ \vdots \\ I(M) \end{bmatrix} = \begin{bmatrix} \tilde{P}_1(1) & \tilde{P}_2(1) & \tilde{P}_3(1) & \tilde{P}_4(1) \\ \vdots & \vdots & \vdots & \vdots \\ \tilde{P}_1(M) & \tilde{P}_2(M) & \tilde{P}_3(M) & \tilde{P}_4(M) \end{bmatrix} \cdot \begin{bmatrix} h_1 \\ h_2 \\ h_3 \\ h_4 \end{bmatrix} = P \cdot \begin{bmatrix} h_1 \\ h_2 \\ h_3 \\ h_4 \end{bmatrix} \quad (4)$$

$$\begin{bmatrix} Q(1) \\ \vdots \\ Q(M) \end{bmatrix} = \begin{bmatrix} \tilde{P}_1(1) & \tilde{P}_2(1) & \tilde{P}_3(1) & \tilde{P}_4(1) \\ \vdots & \vdots & \vdots & \vdots \\ \tilde{P}_1(M) & \tilde{P}_2(M) & \tilde{P}_3(M) & \tilde{P}_4(M) \end{bmatrix} \cdot \begin{bmatrix} n_1 \\ n_2 \\ n_3 \\ n_4 \end{bmatrix} = P \cdot \begin{bmatrix} n_1 \\ n_2 \\ n_3 \\ n_4 \end{bmatrix} \quad (5)$$

where $\tilde{P}_i(t)$ are the output powers whose average values has been subtracted to eliminate the DC-offset distortion. The calibration constants are determined using a deterministic least mean square (LMS) algorithm as follows:

$$\begin{bmatrix} h_1 \\ h_2 \\ h_3 \\ h_4 \end{bmatrix} = \left(P^T \cdot P\right)^{-1} \cdot P^T \cdot \begin{bmatrix} I(1) \\ \vdots \\ I(M) \end{bmatrix} \quad (6)$$

$$\begin{bmatrix} n_1 \\ n_2 \\ n_3 \\ n_4 \end{bmatrix} = \left(P^T \cdot P\right)^{-1} \cdot P^T \cdot \begin{bmatrix} Q(1) \\ \vdots \\ Q(M) \end{bmatrix} \tag{7}$$

I-Q components of the data sequence, received after the training sequence, are recovered applying the calculated eight calibration constants in (1)–(2). However, eight constant values may not be enough to characterize the system, especially for wide-band applications. Radio frequency architectures for SDR require broadband capabilities to operate in multiple bands with multiple standards, and broadband designs do not present a constant or flat response over their large bandwidth. Reflections provoked by mismatches between the components can produce a ripple over the response, which, in the case of the six-port receiver, could be also caused by the variations of the diode coefficients. Future high data rates communication systems will operate with broadband signals, and the I-Q components recovery from eight constant values could not be accurate enough.

To solve this problem we propose an auto-calibration method based on digital channelization. The method consists of separating the signal in sub-bands in the digital domain, and calculating the calibration constants at each band separately and simultaneously. Although the concept of digital channelization seems simple, in a communication system it must be done in real-time, so a computationally efficient filtering is needed. We have selected a particular family of FIR (Finite Impulse Response) type filters for this purpose. The number of filters of the family, N, coincides with the order of each filter. The coefficients, b_k, of each filter, i, are:

$$b_k^i = \frac{1}{N} e^{j(i-1)\frac{2\pi}{N}k} \tag{8}$$

with $k = 0, \ldots, N$ and $i = 1, \ldots, N$. Note that the coefficients of the first filter, b_k^1, are all one (corrected by a $1/N$ factor to normalize the filter gain), and the coefficients of the other filters are equal to b_k^1 but with phase shifts that are integer multiples of $2\pi/N$ radians. This means that the first filter is an Nth-order low-pass filter, and the other filters are equal to the first one but shifted an integer multiple of $2\pi/N$ rad/sample. Each filter has a null response at the central pulsation of the other filters. Therefore, the spectrum is divided into N sub-bands using a small number of coefficients, so the required operations can be performed by the hardware in a real time processing. Let us consider the family of four filters, whose frequency response is

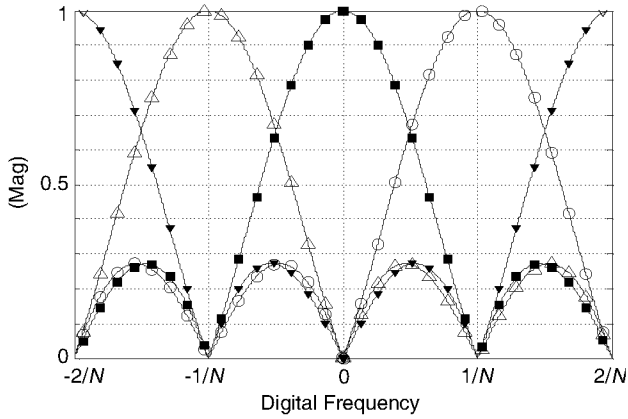

Figure 5. Frequency response of the family of $N = 4$ filters.

shown in Figure 5. The coefficients of the four filters are:

$$b_k^1 = [\ 1 \quad 1 \quad 1 \quad 1\ ] \tag{9}$$

$$b_k^2 = [\ 1 \quad -j \quad -1 \quad -j\ ] \tag{10}$$

$$b_k^3 = [\ 1 \quad -1 \quad 1 \quad -1\ ] \tag{11}$$

$$b_k^4 = [\ 1 \quad -j \quad -1 \quad j\ ] \tag{12}$$

In this case, central digital pulsations are 0, $\pm\pi/2$ and $\pm\pi$ rad/sample; and the coefficients are equal to b_k^1 but shifted $\pm\pi/2$ and $\pm\pi$ rad. This characteristic is especially interesting, as it means that multiplications are not necessary. The required operations reduce just to sums and subtractions, speeding up the signal processing. Indeed, a $\pm\pi$ rad phase shift means just to subtract the sample, and a $\pm\pi/2$ rad phase shift means to exchange the real part for the imaginary part and to sum/subtract.

It can be demonstrated that the sum of every filter response forms an all pass filter. Then, the I-Q components of every sub-band can be added up to obtain the overall I-Q components of the original signal. Therefore, signals coming from the four six-port receiver outputs are filtered, and the calibration constants of every sub-band are simultaneously calculated from (6)–(7). I-Q components at each sub-band are obtained applying the corresponding calibration constants into (1)–(2). Finally, adding the I-Q components of every sub-band, the I-Q components of the original signal are obtained. Figure 6 represents the scheme of the channelized auto-calibration method for $N = 4$. The proposed method can be also combined with adjacent channel rejection techniques, as that described in [18].

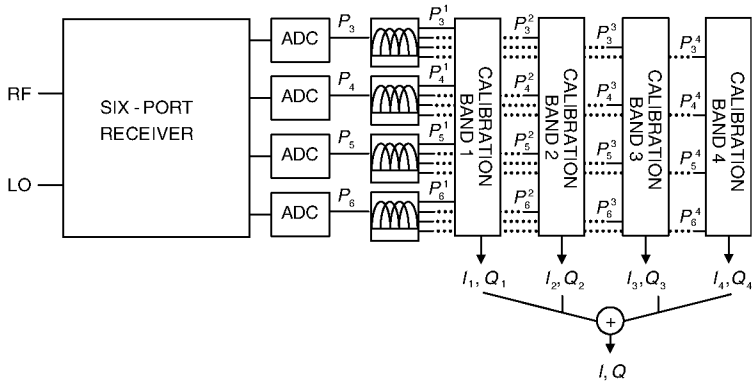

Figure 6. Scheme of the channelized auto-calibration method.

5. MEASUREMENT RESULTS

This section presents the validation of the developed six-port receiver, and the proposed channelized auto-calibration method. The quality of the demodulated signal will be measured in terms of the Error Vector Magnitude (EVM), which is a common figure of merit in digital communications [19]. It is defined as the root-mean-square value of the difference between the measured and ideal symbols, that is:

$$\mathrm{EVM}(\%) = \sqrt{\frac{\frac{1}{N}\sum_{n=1}^{N}|X_{r,n}-X_{i,n}|^2}{\frac{1}{N}\sum_{n=1}^{N}|X_{i,n}|^2}}\cdot 100 \tag{13}$$

where $X_{r,n}$ is the normalized received nth symbol, $X_{i,n}$ is the ideal normalized constellation point of the nth symbol, and N is the number of symbols over which the EVM is calculated.

The test bench is shown in Figure 7. The Agilent E4438C ESG Vector Signal Generator (VSG) generates the RF modulated signal. The LO is the Agilent synthesized sweeper 83752A. Both generators are phase locked. The output signals of the six-port receiver are acquired by a four-channel oscilloscope (Agilent Infiniium), with an over-sampling ratio OSR = 8. The auto-calibration and I-Q regeneration software, implemented in *Matlab*, is applied in a personal computer, and the EVM is calculated using (13). The software does not include any diode linearization technique.

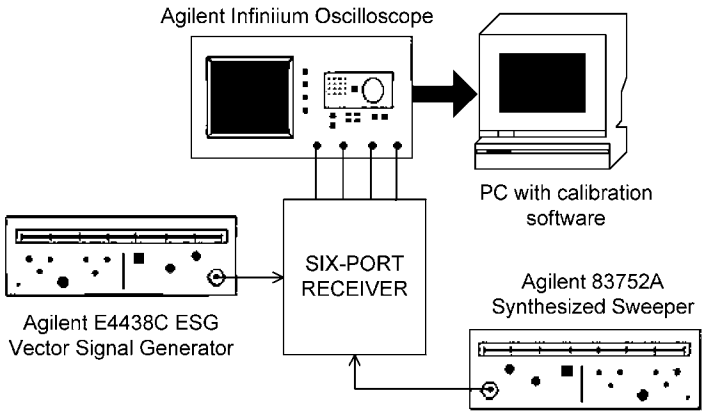

Figure 7. Set-up of the six-port receiver test-bench.

5.1. Validation of the Channelized Auto-calibration Method

In order to validate the described method, we use a 2.45 GHz RF signal with a filtered 64-QAM modulation ($\alpha = 0.3$ roll-off square-root-raised cosine filter). The six-port receiver demonstrator can operate with up to 100 MHz-wide signals, so it is expected to perform symbol rates of about 100 Msymbols/s. However, the Agilent E4438C VSG limits the symbol rate to 12.5 Msymbols/s (75 Mbps) for OSR = 8. The LO power is $P_{\mathrm{LO}} = 0\,\mathrm{dBm}$, and the RF power ($P_{in}$) varies from -45 to $-5\,\mathrm{dBm}$. After the acquisition of 9200 symbols (73600 samples, OSR = 8), we process the data as bursts of length 200 symbols. We use the first 50 symbols to auto-calibrate the system at each burst, and then we demodulate the data sequence of length 150 symbols.

It is advisable to use families with few filters, as it entails few coefficients and thus filtering operations can be real-time performed by the hardware. A lower number of filters can be used by means of previous downsampling. We have used a downsampling ratio of 2, so downsampling and filtering with N filters is similar to use $2N$ filters without downsampling, except for a slight worsening for low input powers due to the noise aliasing provoked by the downsampling. Nevertheless, this could be solved by applying a simple anti-aliasing pre-filtering technique, consisting of forming a decimated version of the signal summing the samples of the original sequence in twos (presumming technique). This is equivalent to use a low-pass second-order FIR filter whose coefficients are equal to one followed by a downsampling with a ratio of 2.

We have compared the EVM obtained from the conventional auto-calibration method (Conventional AM), with no sub-band

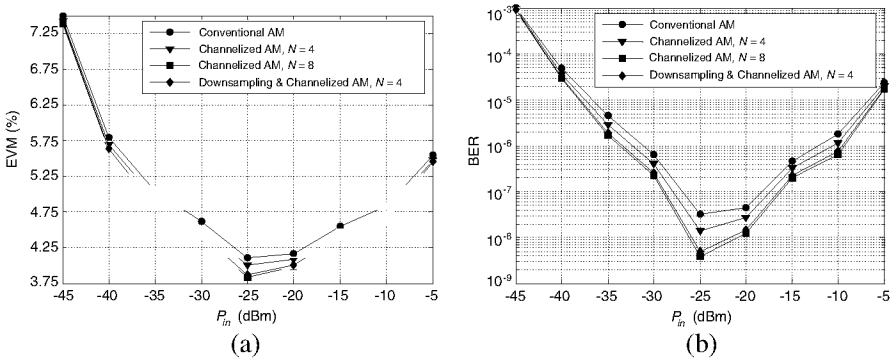

Figure 8. Validation of the channelized auto-calibration method: 75 Mbps 64-QAM, 2.45 GHz. (a) Measured EVM versus P_{in}. (b) BER calculated from EVM.

division [18], to that obtained from our proposed channelized auto-calibration method (Channelized AM), with and without downsampling. Figure 8(a) shows the measured EVM as a function of P_{in}. Take into account that neither a LNA nor an AGC have been included in the receiver. EVM curves show quality degradation for high levels of P_{in} due to the rectified wave, a baseband term superposed to the desired signal that increases quadratically with the signal power and, therefore, produces more degradation for high power levels [11]. The results show significant EVM improvements, up to 0.3 percentage points with respect to conventional AM for $N = 8$ filters or $N = 4$ with downsampling. For a Gaussian noise model and a number of received symbols greater than the alphabet length, EVM and signal to noise ratio (SNR) are related by the expression [19]:

$$\mathrm{SNR} \approx \frac{1}{\mathrm{EVM}^2} \tag{14}$$

From (14), we can obtain the BER (Bit Error Ratio) curves represented in Figure 8(b). A maximum BER improvement of about one order of magnitude is achieved with $N = 8$ filters or $N = 4$ with downsampling. The channelized auto-calibration method is specially suited for broadband communications and strict QoS (Quality of Service) requirements, but it is not useful for reducing the sensitivity. The BER reduction is significant with few filters, but if best results are desired, there will be a trade-off between BER reduction and computational efficiency. The use of the proposed channelized auto-calibration method with only four filters introduces an improvement of 8 dB in the dynamic range of a receiver subject to a BER $= 10^{-6}$

specification. This is an important advantage of the method, as multi-port schemes do not present good dynamic range behaviour [5].

Obviously, the benefits of the auto-calibration method will be more significant for wideband signals and strong system imbalances, although we can not experimentally prove it because of the test instruments limitations. To demonstrate it, we have simulated the performance of a six-port receiver composed of a six-port network, four power detectors and four low-pass filters. The input signal is the complex envelope of a 64-QAM modulated signal ($\alpha = 0.3$) with a bit rate of 420 Mbit/s, combined with an additive white Gaussian noise (AWGN). The OSR is 8. The LO power is 0 dBm, and the RF power varies from -70 to -10 dBm. Power detectors present square law behaviour and the low-pass filters have ideal responses. The six-port network topology is that shown in Figure 2. We have introduced different ripples over the nominally magnitude and phase parameters of each output port: between 2.5 and 3 dB in magnitude, and 1° and 6° in phase. These ripples have been modelled as sine type functions with a fast frequency variation, in order to validate the auto-method under critical conditions. The simulated BER curves versus SNR are presented in Figure 9. Notice that simulated BER curves respond to the real curves tendency observed in Figure 8. On one hand, no significant BER improvements are achieved for low values of SNR. The effect of the noise aliasing when the downsampling is applied can clearly be appreciated in Figure 9. On the other hand, it can be seen the increase in BER for high input power levels due to the rectified wave. And finally, the BER improvement is maximized when the dominant source of distortion responds to system imbalances (SNR = 40 dB).

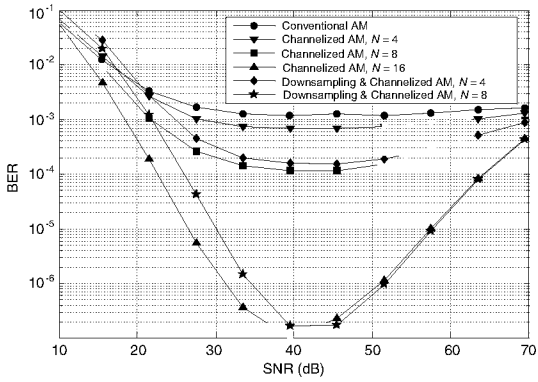

Figure 9. Simulated BER versus SNR for a 420 Mbps 64-QAM signal and strong six-port frequency response variations.

As it happened in the experimental validation, BER improvements of about one order of magnitude are achieved with $N = 8$ filters or $N = 4$ with downsampling. Using $N = 16$ filters or $N = 8$ with downsampling, a BER below 10^{-6} is reached, since the original BER value of 10^{-3} obtained with the conventional AM.

5.2. Multi-mode and Multi-band Behaviour

With the purpose of demonstrating the multi-mode and multi-band characteristics of the SDR six-port receiver, we have measured the EVM for different modulation schemes and frequency bands. We have selected several frequencies corresponding to communication standards, such as GSM (900 MHz, 1800 MHz), PCS (1900 MHz), Wi-Fi (2.45 GHz), or WiMAX (700 MHz, 3500 MHz, 5800 MHz). The modulation schemes are QPSK, 16-QAM, and 64-QAM. The LO power is fixed to $P_{\mathrm{LO}} = 0\,\mathrm{dBm}$, and the input power is $P_{in} = -20\,\mathrm{dBm}$. For frequencies below 3 GHz, we have changed the VSG for the Agilent N5182A MXG, which can provide a symbol rate of 15.625 Msymbol/s for OSR = 8. Therefore, it is possible to achieve a bit rate of 93.75 Mbps for a 64-QAM modulation. In all cases, we have acquired a total of 1000 symbols, which have been processed as bursts of length 200 symbols. The first 50 symbols of each burst are used for calibrating. We have applied the channelized auto-calibration method with $N = 4$ filters and previous downsampling (downsampling ratio of 2). The measured values of EVM are presented in Table 1.

These results show a good performance of the six-port receiver

Table 1. Measured EVM, $P_{\mathrm{LO}} = 0\,\mathrm{dBm}$, $P_{in} = -20\,\mathrm{dBm}$.

Frequency (MHz)	Modulation	Bit Rate (Mbps)	EVM (%)
300	64-QAM	75	6.1
700	16-QAM	62.5	4.8
900	64-QAM	93.75	4.7
1800	QPSK	31.25	4.7
1900	16-QAM	62.5	4.6
2450	64-QAM	93.75	4.5
3500	16-QAM	50	4.4
4000	QPSK	25	4.5
5800	64-QAM	75	4.3
6000	QPSK	25	4.4

for high data rates over a four-octave frequency range. As it was previously stated in Section 3, the operating frequency range of the six-port network could be enlarged due to its good frequency response. The results shown in Table 1 demonstrate that the six-port operating range can be extended from 300 MHz to 6 GHz (4.32 octaves) with good performance, although it was designed to cover the frequencies from 698 MHz to 5850 MHz. From theoretical analysis based on the measured six-port response, it is derived that the six-port operation could be extended also beyond 6 GHz. However, it has not been experimentally demonstrated due to test equipment limitations.

5.3. Influence of the LO Power

An important advantage of the six-port architecture is its operation with low LO power levels. This means low power consumption, better RF-LO isolation, and reduction of the LO self-mixing, which is one of the main problems of zero-IF architectures. On the contrary, mixers used in conventional zero-IF receivers require high LO powers.

In order to demonstrate this characteristic, we have measured the EVM for different values of P_{LO}, keeping the input power level at $P_{in} = -20\,\mathrm{dBm}$. We use a 1.8 GHz 25 Mbps QPSK modulated signal ($\alpha = 0.3$). A total of 1000 symbols (8000 samples, OSR = 8) are acquired with the oscilloscope. The first 50 symbols of each data burst (length 200 symbols) are used to auto-calibrate the system and regenerate the IQ components of the next 150 data symbols. We apply the channelized auto-calibration method with $N = 4$ filters and previous downsampling (downsampling ratio of 2). Figure 10 shows the constellation diagrams of the demodulated signal. The obtained values of EVM are: 4.4% for $P_{\mathrm{LO}} = 10\,\mathrm{dBm}$; 4.8% for $P_{\mathrm{LO}} = 0\,\mathrm{dBm}$; 5.1% for $P_{\mathrm{LO}} = -10\,\mathrm{dBm}$; and 6.3% for $P_{\mathrm{LO}} = -20\,\mathrm{dBm}$. These results prove that six-port receivers can operate for low LO power values.

Nevertheless, a suitable selection of the LO power level is required. A study of the optimal LO power for maximizing the SNR at the baseband outputs is presented in [20]. When the phase noise contribution is not considered, thermal and shot noises are the dominant sources of distortion, and a maximum SNR of 33 dB is achieved for LO powers in the range of 3–7 dBm. Considering the phase noise contribution, the maximum value of SNR, corresponding to a LO power range from −7 to −2 dBm, decreases 14 dB. However, the maximum diode conversion efficiency is achieved for high LO power levels, around 13 dBm. These figures are obtained from the simulation results of [20], although similar values would be obtained in our case. The spurious signal rejection as a function of the LO power must also be considered.

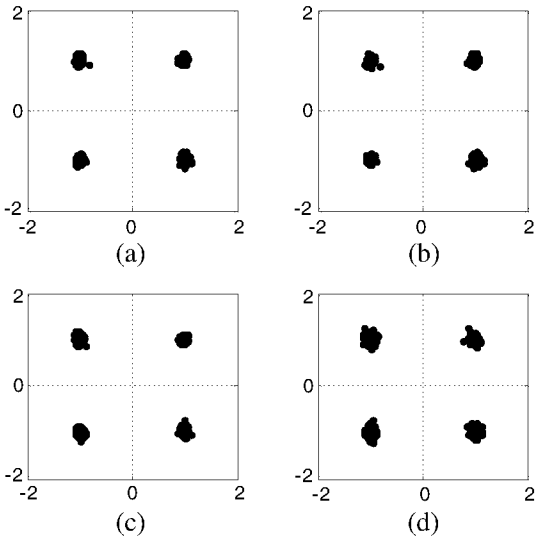

Figure 10. Constellation diagrams for 25 Mbps QPSK, 1.8 GHz, $P_{in} = -20$ dBm. (a) $P_{\mathrm{LO}} = 10$ dBm. (b) $P_{\mathrm{LO}} = 0$ dBm. (c) $P_{\mathrm{LO}} = -10$ dBm. (d) $P_{\mathrm{LO}} = -20$ dBm.

5.4. Comparison of Multi-port Demodulators

To conclude, the comparison with other multi-port demodulators operating in the frequency range of interest is presented in Table 2. As the quality of the demodulated signal is evaluated in terms of EVM or BER, we provide the theoretical BER versus EVM curves for QPSK, 16-QAM and 64-QAM modulation schemes in Figure 11 [19].

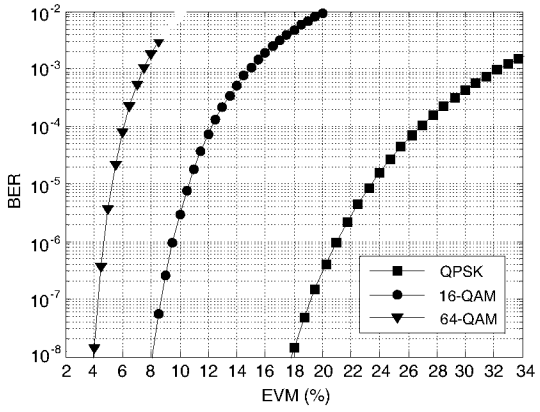

Figure 11. Theoretical BER versus EVM curves.

Table 2. Comparison of multi-port demodulation performances.

Ref.	Operating	Measurement results				
		Data signal	P_{LO} **(dBm)**	P_{in} **(dBm)**	**Freq. (GHz)**	**Quality of demodulated signal**
[21] (2003)	0.9–5	97.2 kbps QPSK	0	−20	0.9–4	EVM < 14%
[18] (2004)	2–3	200 kbps QPSK	0	−62.5	2	BER = 10^{-3}
[22] (2006)	2–9.4	8PSK	-	−19	2.4	Not quantified
				−27	5.8	
				−31	9.4	
[23] (2006)	0.9–4	1 Mbps QPSK	−10	−15	2.45	EVM = 12%
[24] (2008)	3.1–4.8	1 Mbps QPSK	−1.5	-	3.432	EVM = 5.5%
					3.96	EVM = 4%
					4.488	EVM = 6.3%
[25] (2009)	0.8–2.4	4 Mbps 16-QAM	−8.5	−33.3 to −2.6	0.8	BER < 10^{-3}
				−39.6 to −0.6	1.6	
				−38 to −0.7	2.4	
				≈ −32	1.6	BER = 10^{-6}
[26] (2010)	0.9–4	400 kbps QPSK	−10	−20	2.45	EVM = 5.9%
				−40		EVM = 7.9%
[27] (2011)	7–8	1.67 Gbps 16 QAM	15	−15	7.5	EVM = 10.9%
This work	0.3–6	75 Mbps 64-QAM	0	−20	0.3	EVM = 6.1%
		62.5 Mbps 16-QAM	0	−20	0.7	EVM = 4.8%
		93.75 Mbps 64-QAM	0	−20	2.45	EVM = 4.5%
		25 Mbps QPSK	0	−20	6	EVM = 4.4%
			−20		1.8	EVM = 6.3%

The six-port receiver is said to be a good solution for the multi-band demodulation of high-speed signals, but no many experimental demodulation results proving both assumptions have been published up to now. Some published works are not strictly multi-band [18, 24]; other are multi-band but only validate the demodulator for a single frequency [23, 26]; and other prove the multi-band behaviour but do not quantify the quality of the demodulated signal [22]. In [21, 25] the demodulation performance is quantified over the entire operating frequency range, but with data rates much lower than in our experiments. Recently, a six-port demodulator supporting a 1.67 Gbps data rate has been published [27]. However, this is not a broadband design, as it only covers the range from 7 to 8 GHz. In addition, the measured EVM is quite high, even though the high LO power level (15 dBm). Our six-port receiver has been validated over a four octave bandwidth (0.3–6 GHz), and for up to 93.75 Mbps data rates with low values of EVM. It outperforms the other designs in terms of bandwidth and quality of the demodulated signal.

6. CONCLUSION

In this paper we have introduced a SDR 0.3–6 GHz six-port receiver for broadband and high data rates applications. The six-port receiver has been measured with good performance over the frequencies of the main communication standards up to 6 GHz. The prototype has been validated for data rates of 93.75 Mbps (limited by the test instruments), although it has been designed to operate with 100 MHz instantaneous bandwidth, so a bit rate of 600 Mbps for a 64-QAM modulation is foreseen. Our work demonstrates empirically and quantitatively the multi-band behaviour of the six-port architecture, and the capability of performing high data rates.

A new auto-calibration method based on a computational efficient sub-band division for broadband applications has been described. The method is specially suited for broadband communications and strict QoS requirements. The proposed FIR filters are easy to implement and have few coefficients, so operations can be real-time performed by the hardware. In addition, operations can be reduced to sums and subtractions using four filters, speeding up the signal processing. Measurement results show a significant BER improvement, above one order of magnitude with respect to conventional auto-calibration method.

Currently, our efforts are focused on the development of an LTCC version of the six-port receiver, with the purpose of miniaturizing the design.

ACKNOWLEDGMENT

This work has been funded by the Spanish National Board of Scientific and Technological Research (CICYT), under project contract TEC2008–02148, and by INDRA SISTEMAS, under TelMAX project inside CENIT program.

REFERENCES

1. Mitola, J., "The software radio architecture," *IEEE Commun. Mag.*, Vol. 33, No. 5, 26–38, 1995.
2. Abidi, A. A., "The path to the software-defined radio receiver," *IEEE J. Solid-State Circuits*, Vol. 42, No. 5, 954–966, 2007.
3. De la Morena-Álvarez-Palencia, C., M. Burgos-García, and D. Rodríguez-Aparicio, "Software defined radio technologies for emergency and professional wide band communications," *IEEE Int. Carnahan Conf. Security Tech.*, 357–363, San Jose, CA, 2010.
4. Luy, J. F., T. Mueller, T. Mack, and A. Terzis, "Configurable RF receiver architectures," *IEEE Microw. Mag.*, Vol. 5, No. 1, 75–82, 2004.
5. Wu, K., "Multiport interferometer techniques for innovative transceiver applications," *IEEE Radio and Wireless Symp.*, 531–534, New Orleans, LA, Jan. 2010.
6. Bosisio, R. G., Y. Y. Zhao, X. Y. Xu, S. Abielmona, E. Moldovan, Y. S. Xu, M. Bozzi, S. O. Tatu, C. Nerguizian, J. F. Frigon, C. Caloz, and K. Wu, "New-wave radio," *IEEE Microw. Mag.*, Vol. 9, No. 1, 89–100, 2008.
7. Koelpin, A., G. Vinci, B. Laemmle, D. Kissinger, and R. Weigel, "The six-port in modern society," *IEEE Microw. Magazine*, Vol. 11, No. 7, 35–43, Dec. 2010.
8. Hammou D., E. Modovan, and S. O. Tatu, "Modelling and analysis of a modified V-band MHMIC six-port circuits," *Journal of Electromagnetic Waves and Applications*, Vol. 24, No. 10, 1419–1427, 2010.
9. Khaddaj Mallat, N., E. Moldovan, and S. O. Tatu, "Comparative demodulation results for six-port and conventional 60 GHz direct conversion receivers," *Progress In Electromagnetics Research*, Vol. 84, 437–449, 2008.
10. Engen, G. F., "The six-port reflectometer. An alternative network analyzer," *IEEE Trans. Microw. Theory Tech.*, Vol. 25, No. 12, 1075–1080, 1977.

11. Hentschel, T., "The six-port as a communications receiver," *IEEE Trans. Microw. Theory Tech.*, Vol. 53, No. 3, 1039–1047, 2005.
12. De la Morena-Álvarez-Palencia, C., M. Burgos-García, and D. Rodríguez-Aparicio, "Three octave six-port network for a broadband software radio receiver," *European Microwave Conf.*, 1110–1113, Paris, France, Sep. 2010.
13. Kaliouby, L. and R. G. Bosisio, "A new method for six-port swept frequency automatic network analysis," *IEEE Trans. Microw. Theory Tech.*, Vol. 32, No. 12, 1678–1682, 1984.
14. Alkanhal, M. A. S., "Dual-band bandpass filter using inverted stepped-impedance resonators," *Journal of Electromagnetic Waves and Applications*, Vol. 23, No. 8–9, 1211–1220, 2009.
15. Lin, X. M., "Design of compact tri-band bandpass filter using $\lambda/4$ and stub-loaded resonators," *Journal of Electromagnetic Waves and Applications*, Vol. 24, No. 14–15, 2029–2035, 2010.
16. Weng, R. M. and P. Y. Hsiao, "Double-layered quad-band bandpass filter for multi-band wireless systems," *Journal of Electromagnetic Waves and Applications*, Vol. 23, No. 16, 2153–2161, 2009.
17. Li, L. and D. Uttamchandani, "Demonstration of a tuneable RF MEMS band-pass filter using silicon foundry process," *Journal of Electromagnetic Waves and Applications*, Vol. 23, No. 2–3, 405–413, 2009.
18. Neveux, G., B. Huyart, and G. J. Rodriguez-Guisantes, "Wideband RF receiver using the "five-port" technology," *IEEE Trans. Vehicular Technology*, Vol. 53, No. 5, 1441–1451, 2004.
19. Shafik, R. A., S. Rahman, R. Islam, and N. S. Ashraf, "On the error vector magnitude as a performance metric and comparative analysis," *Int. Conf. Emerging Technologies, Peshawar, Pakistan*, 27–31, Nov. 2006.
20. Winter, S. M., H. J. Ehm, A. Koelpin, and R. Weigel, "Six-port receiver local oscillator power selection for maximum output SNR," *IEEE Radio and Wireless Symp.*, 151–154, Jan. 2008.
21. Xiong, X. Z. and V. F. Fusco, "Wideband 0.9 GHz to 5 GHz six-port and its application as digital modulation receiver," *IET Proc. Microw. Antennas Propag.*, Vol. 150, No. 4, 301–307, 2003.
22. Tatu, S. O., K. Wu, and T. Denidni, "Multiband multiport direct conversion receiver: Design, implementation and demodulation results," *Microw. Optical Technology Lett.*, Vol. 48, No. 4, 817–822, 2006.
23. Haddadi, K., H. El Aabbaoui, C. Loyez, D. Glay, N. Rolland,

and T. Lasri, "Wide-band 0.9 GHz to 4 GHz four-port receiver," *IEEE Int. Conf. Electron. Circuits and Systems*, 1316–1319, Nice, France, Dec. 2006.

24. Hakansson, P. and S. Gong, "Ultra-wideband six-port transmitter and receiver pair 3.1–4.8 GHz," *Asia-Pacific Microw. Conf.*, 1–4, Hong Kong/Macau, China, Dec. 2008.
25. Perez-Lara, P., J. A. Medina-Rodriguez, I. Molina-Fernandez, J. G. Wanguemert-Perez, and A. Gonzalez-Salguero, "Wideband homodyne six-port receiver with high LO-RF isolation," *IET Microw. Antennas Propag.*, Vol. 3, No. 5, 882–888, 2009.
26. Haddadi, K., M. M. Wang, C. Loyez, D. Glay, and T. Lasri, "Four-port communication receiver with digital IQ-regeneration," *IEEE Microw. Wireless Compon. Lett.*, Vol. 20, No. 1, 58–60, 2010.
27. Östh, J., A. Serban, Owais, M. Karlsson, S. Gong, J. Haartsen, and P. Karlsson, "Six-port gigabit demodulator," *IEEE Trans. Microwave Theory Tech.*, Vol. 59, No. 1, 125–131, Jan. 2010.